UCRL-JC-124875
PREPRINT

Effect of SiO_2 overcoat thickness on laser damage morphology of HfO_2/SiO_2 Brewster's angle polarizers at 1064 nm

C. J. Stolz, F. Y. Génin, T. A. Reitter, N. E. Molau, R. P. Bevis, M. K. von Gunten, D. J. Smith, and J. F. Anzellotti

This paper was prepared for submittal to the 28th Annual Symposium on Optical Materials for High Power Lasers Boulder, Colorado October 7-9, 1996

March 3, 1997

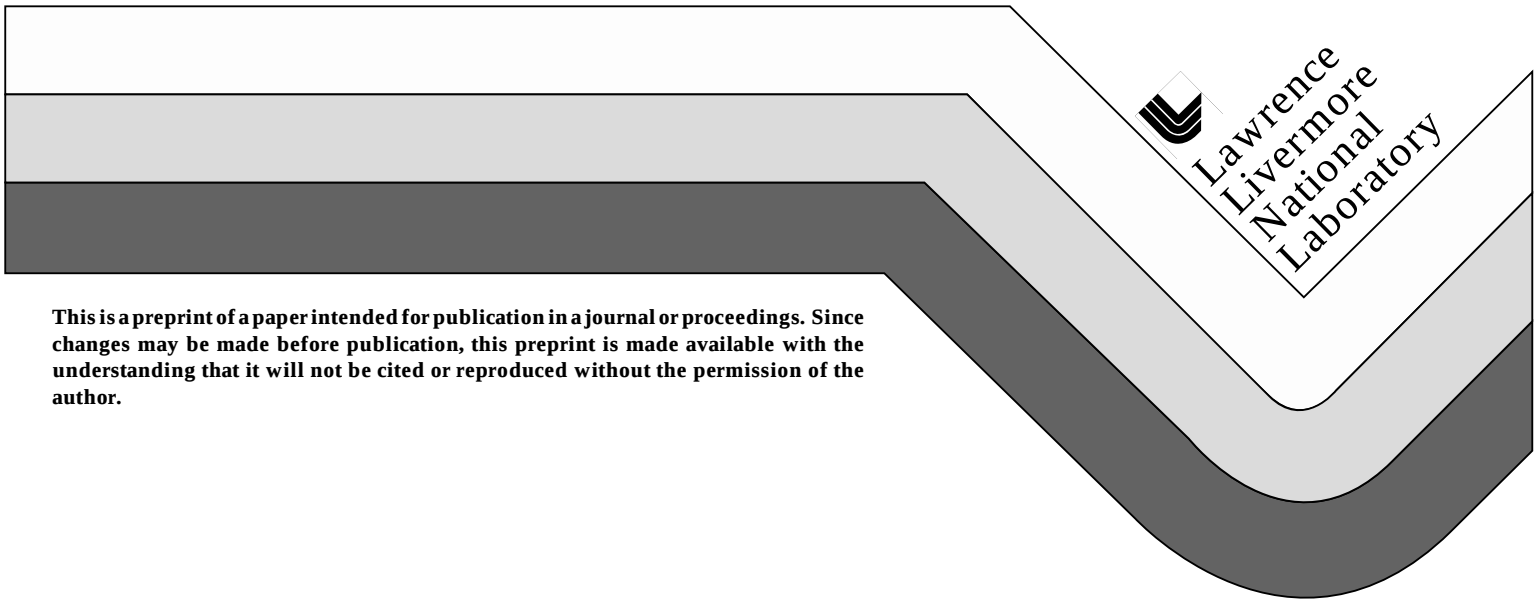

Effect of SiO_2 overcoat thickness on laser damage morphology of HfO_2/SiO_2 Brewster's angle polarizers at 1064 nm

C. J. Stolz, F. Y. Génin, T. A. Reitter, N. E. Molau
University of California
Lawrence Livermore National Laboratory
P. O. Box 808, L-487
Livermore, CA 94550

R. P. Bevis, M. K. von Gunten
Spectra-Physics Lasers, Inc.
Components and Accessories Group
P.O. Box 7013
Mountain View, CA 94943

D. J. Smith, J. F. Anzellotti
University of Rochester
Laboratory for Laser Energetics
250 East River Road
Rochester, NY 14623

ABSTRACT

HfO_2/SiO_2 Brewster's angle polarizers are being developed at Lawrence Livermore National Laboratory for the National Ignition Facility. Damage threshold studies using a 3-ns pulse length 1064-nm laser have revealed a number of different damage morphologies such as nodular ejection pits, plasma scalds, flat bottom pits, and overcoat delaminations. Of these laser damage morphologies, delaminations have the most negative impact on the multilayer stability. By selecting the proper SiO_2 overcoat thickness, the delamination morphology is eliminated without significantly modifying the spectral characteristics of the coating and the functional damage threshold is increased by 2-4×. A model of the thermal mechanical response of the overcoats is presented for various SiO_2 overcoat thicknesses. The overcoat thickness influences the electric-field profile resulting in different thermal gradients between the outer SiO_2 and HfO_2 layers. This modeling effort attempts to understand the relationship between the thermal stress distribution in the overcoat and the occurrence of delamination.

Key words: laser-induced damage, hafnia-silica polarizers, laser damage morphology, electric-field distribution, thermal gradients, stress gradients, silica overcoat

1. INTRODUCTION

The National Ignition Facility (NIF) requires 192 large area (0.34 m^2) polarizers that must survive peak fluences of 10.5 J/cm^2 for 1053-nm 3-ns Gaussian pulses. The function of these polarizers are different than past fusion laser systems due to a significant departure in the NIF laser architecture.[1] Previous fusion lasers used polarizers to isolate the transmitted pulse to prevent gain of unwanted pulses. In the NIF laser, the polarizer serves the dual function of isolating unwanted pulses and reflecting the pulse out of a multiple-pass amplifier after sufficient amplification has been achieved. Therefore the polarizer is not limited by the low laser fluence of the "P" polarized transmitted beam, but the high fluence of the "S" polarized reflected beam. Unlike high reflectors, the performance limiting damage morphology of polarizers is delamination of the overcoat.[2,3]

SiO_2 overcoats of various thicknesses have been documented to increase the damage threshold and modify the damage morphology of HR coatings.[4-14] Although this technique has been known for over 20 years, there has been little theoretical understanding of the resultant damage threshold improvement. Traditionally, the overcoat optical thickness is a halfwave, or an absentee layer, to maintain the coating's spectral characteristics at the design wavelength. The electric-field profile of the reflector stack is unchanged while the peak electric field, now centered in the overcoat, is substantially greater than peaks in the high reflector stack.[5] This result implies that the damage mechanism is not influenced by the electric field in the overcoat. It has also been suggested that overcoats improve the mechanical properties of the thin film,[6,11] but laser damage thresholds are improved for coatings with either SiO_2 and MgF_2 overcoats implicating an alternate mechanism because these materials are mechanical antitheses.[6,10] Results from investigations of overcoats by time resolved pulsed photothermal

deflection and cw-photothermal microscopy suggest that laser damage initiates in the outer high refractive index layer and that higher thermal conductivity in the overcoat than air plays a significant role in the damage mechanism as well as reduces and smoothes the peak temperatures of localized absorption centers in the outer high refractive index layer.[13]

Little work has been done to understand the role of overcoat thickness on the laser-induced damage of Brewster's angle thin film plate polarizers. Traditionally the SiO_2 overcoat thickness of a polarizer is dictated by the requirement that the outer layers are an antireflection coating between the incident medium and the reflector stack to achieve high transmission in "P" polarization. To increase the manufacturing yield of polarizers, the coatings are designed for maximum polarizing region bandwidth. An additional halfwave thickness to the overcoat slightly reduces the polarization bandwidth and increases the reflected wavefront distortion by increasing the coating stress. Recent tests on polarizers with thin SiO_2 overcoats demonstrate a significant relationship between incident angle and laser damage morphology type.[15] By changing the incident angle, hence the electric field, temperature, and stress profile, overcoat delaminations were eliminated. These results suggest that overcoat thickness may play a significant role in eliminating overcoat delaminations due to the impacts of overcoat thickness on the thermomechanical properties of the coating stack.

2. EXPERIMENT

Three different polarizer coating designs, with and without overcoats, were prepared by two different coating vendors. The coatings were deposited by electron-beam deposition from Hf and SiO_2 starting materials. In each design case, the polarizers were deposited in platens that independently mask each substrate during deposition so each coating design was deposited in a single run under identical conditions with the only variation being the overcoat thickness. The first design consisted of SiO_2 overcoats with 0 and $\lambda/2$ optical thicknesses. The second design consisted of SiO_2 overcoats with $\lambda/7$ and $\lambda/7+ \lambda/2$ optical thicknesses. The final design consisted of SiO_2 overcoats with $\lambda/7$, $\lambda/3$, and $\lambda/7+ \lambda/2$ optical thicknesses.

The coatings were damage tested using a raster scan technique similar to the laser conditioning process described by Sheehan et al. and used on large aperture fusion laser coatings.[16] In summary, the optic is translated past a stationary laser beam to raster scan the entire surface of the optic as illustrated in figure 1. By defining the step size between pulses to equal the laser beam diameter at 90% of the peak fluence, the entire surface is exposed to ≥90% of the peak laser fluence. The raster scan damage test used on these samples started with the first scan at 5 J/cm^2 and increased in 5 J/cm^2 increments until massive failure was observed with a 100× magnification Normarski microscope. The fluence measurement uncertainty is ±15%. The LLNL damage test lasers are flash lamp pumped with a Gaussian spatial profile, 3-ns or 8.6-ns pulse length, and 10-Hz repetition rate described elsewhere.[17] The reported fluences are all scaled to 3-ns pulses by $\tau^{0.35}$.

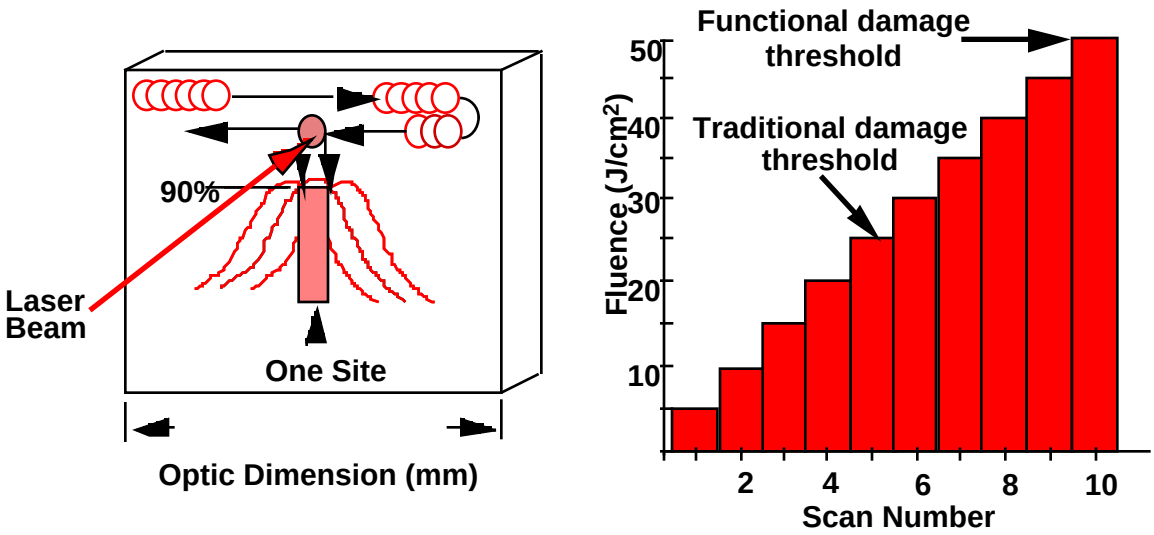

Fig. 1 Raster scan damage test consists of irradiating an entire surface at a single fluence (≥90% of the peak fluence) starting at a low fluence and incrementally increasing the fluence for each subsequent scan until the functional damage threshold is determined. The traditional damage threshold is the fluence where any visible morphological changes to the coating occurs whereas the functional damage threshold is the fluence where any morphological changes to the coating occur that impact laser propagation.

3. RESULTS

The criteria used for coating failure is the functional damage threshold, defined as any laser-induced coating morphological change that limits laser performance, either by catastrophic failure or beam modulations created by the damage site that affect laser propagation.[2,3] This is a significant departure from the traditional laser damage threshold definition, namely, any morphological surface change observed under a defined microscopic condition. It is acknowledged by fusion laser designers that the optical components in NIF will be damaged due to laser irradiation. As long as the laser damage during laser operation does not become massive and remains smaller than a critical size of less than 280 μm, determined by beam propagation codes, the laser performance will not be impacted.[2] Therefore the functional damage threshold is a better criteria for developing coating designs and processes for large aperture high fluence laser coatings.

Four classes of laser damage morphologies are generally observed in HfO_2/SiO_2 polarizers when irradiated with 1064 nm 3-ns pulses.[2-3] They are pits created by nodular defect ejection, plasma scalds or coating surface modification due to the presence of a plasma, flat-bottom pits that occur at the layer interfaces of the first three electric field peaks, and delaminations or removal of the outer layer. The first three classes are relatively benign damage morphologies, while the delaminations are extremely unstable when exposed to additional laser pulses.[3] By eliminating the delamination damage morphology, the functional damage threshold of the coating is increased.

Design 1 (0 and λ/2 SiO_2 overcoat):

The typical laser-induced damage morphology of a polarizer coating without a SiO_2 overcoat is delamination of the outer hafnia layer as illustrated in figure 2 and summarized in table 1. This type of laser damage tends to grow with further irradiation. A very different laser-induced morphology is observed for the same coating with a λ/2 SiO_2 overcoat. The damage tends to be small pits that are most likely the result of ejected nodular defects. Surrounding the pits are plasma scalds or surface modifications caused by the formation of a plasma near the surface during the damage process. The impact of these plasma scalds on beam propagation is not fully characterized, but appears to be benign.[2] Although some pits are created at similar fluences as the delaminations, the pits do not grow in the overcoated sample unless irradiated at a 4× higher fluence.

Design 2 (λ/7 and λ/7 + λ/2 SiO_2 overcoat):

For both overcoat thicknesses, the predominant laser-induced damage morphology are pits, most likely due to nodular ejection, surrounded by plasma scalds as illustrated in figure 3. A few sites on the thinner overcoat damaged massively, making it impossible to determine the origin of the damage. The damage morphologies of the λ/7 + λ/2 overcoat were benign even at the peak fluence of the damage tester, resulting in a greater than 2× increase in the functional damage threshold.

Design 3 (λ/7, λ/3, and λ/7 + λ/2 SiO_2 overcoat):

The damage morphology of the coating with the thinnest overcoat, λ/7, was typically delamination. The λ/3 thickness overcoat damage morphology was deep pitting at what appeared to be nodular defects. The damage morphology of the coating with a λ/7 + λ/2 overcoat are plasma scalds and small pits most likely the result of nodular ejection. Even at the peak operating fluence of the damage tester, all of the damage morphologies were benign, therefore the additional λ/2 overcoat resulted in a greater than 2× increase in the functional damage threshold as illustrated in figure 4.

Table 1 Summary of the functional damage threshold and failure morphology as a function of overcoat thickness for the three evaluated Brewster's angle polarizer designs.

Design	Overcoat thickness	Functional damage threshold (J/cm^2)	Failure morphology
1	0λ	15.8	Delamination
1	λ/2	62.3	Massive
2	λ/7	19.6	Massive
2	λ/7 + λ/2	>40.7	None
3	λ/7	22.6	Delamination
3	λ/3	16.1	Massive
3	λ/7 + λ/2	>47.9	None

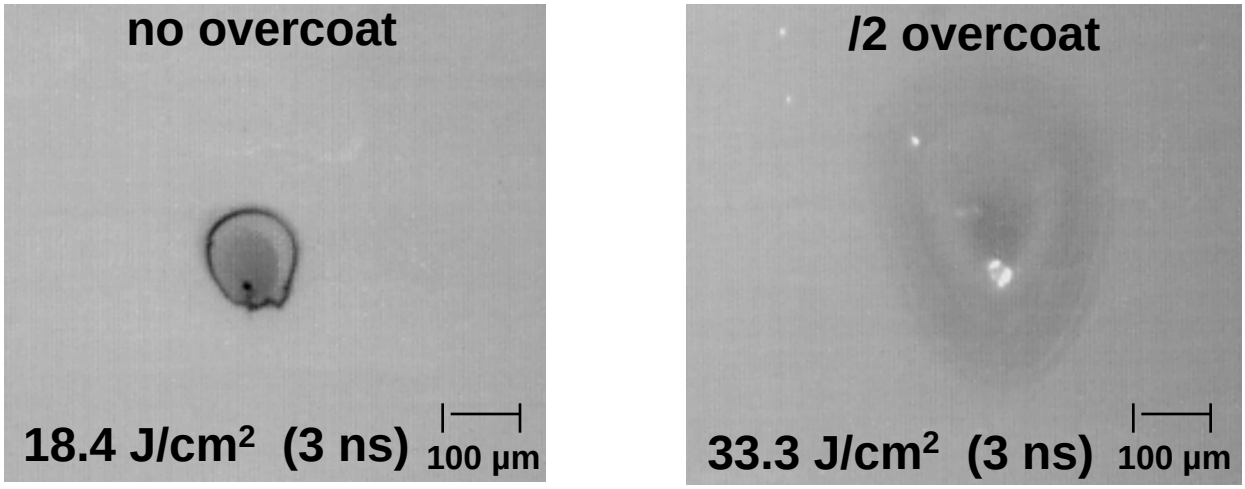

Fig. 2 Design 1: The laser-induced damage morphology is altered significantly due to the presence of a SiO_2 overcoat as indicated by the outer HfO_2 layer delamination for the polarizer without SiO_2 overcoat and pitting and plasma scalds observed in the SiO_2 overcoated sample. The functional damage threshold of this polarizer was increased from 15.8 J/cm^2 to 62.3 J/cm^2 (8.6-ns scaled to 3-ns Gaussian pulse) by the addition of the SiO_2 overcoat.

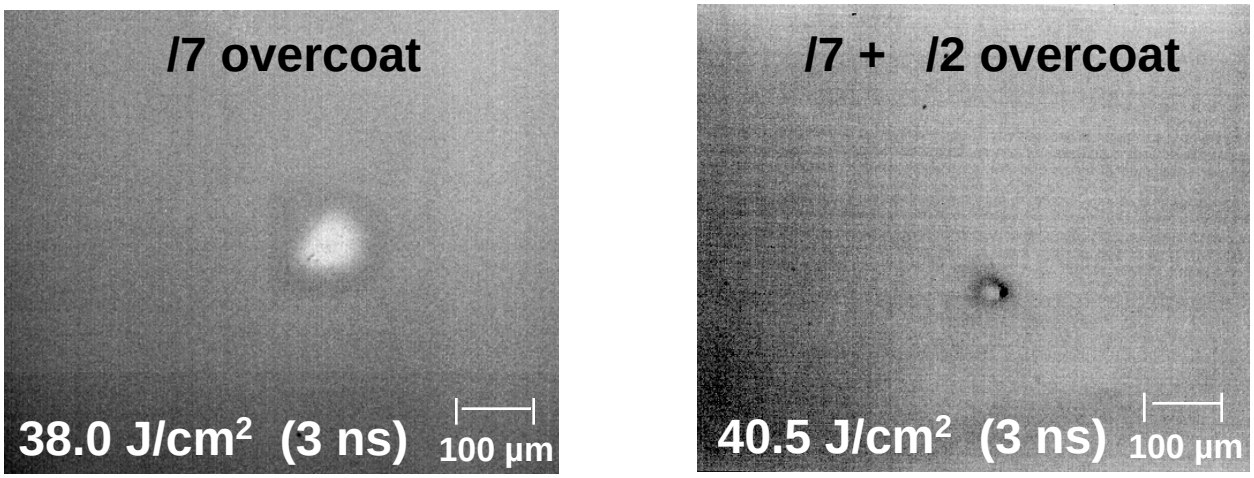

Fig. 3 Design 2: The laser-induced damage morphology is similar for most damage sites for both SiO_2 overcoat thickness, but catastrophic failure occurs at a much lower fluence for the thinner overcoat. The functional damage threshold of this polarizer was increased from 19.6 J/cm^2 to >40.7 J/cm^2 (3-ns Gaussian pulse) by the increasing the thickness of the SiO_2 overcoat.

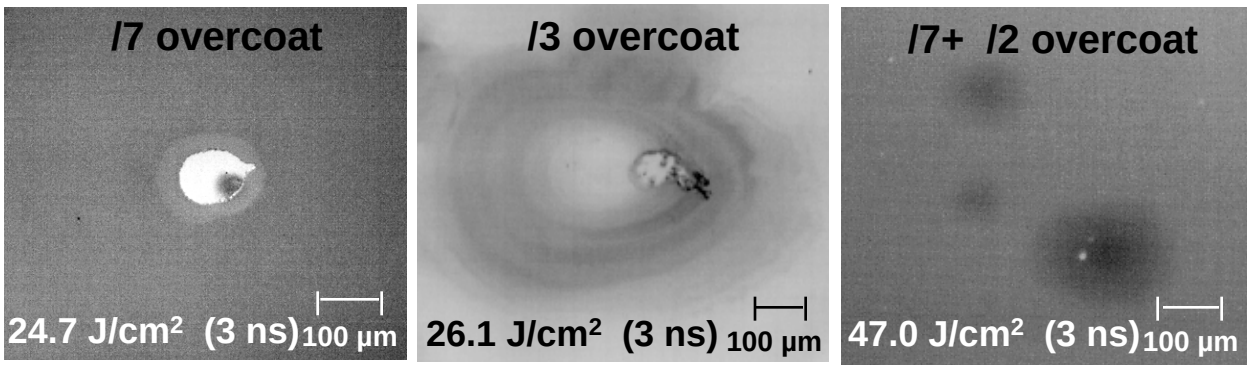

Fig. 4 Design 3: Thicker SiO_2 overcoats eliminated overcoat delamination. Deep pitting was observed for the medium thickness overcoat, probably the result of the high electric field penetration into the coating. The functional damage threshold of this polarizer with increasing overcoat thickness is 22.6, 16.1, and >47.9 J/cm^2 (3-ns Gaussian pulse) respectively.

4. ANALYSIS

To better understand the observed morphologies, electromagnetic and thermomechanical modeling codes were used to evaluate multilayer stability during laser irradiation. Previously, modeling of thermally induced stress has been used to understand laser damage in high reflector coatings with and without nodular defects.[18-20] Modeling of thermally induced stresses has also been successfully applied to understanding the damage morphology of polarizers irradiated at different incident angles.[15] The results of this work implied that by increasing the overcoat thickness, one might be able to eliminate overcoat delamination by decreasing the temperature gradient between the outer two layers. For consistency, the materials properties listed in Table 2 and used in this modeling effort are the same as those previously reported for modeling of nodular defects. Since the accuracy of the materials properties is unknown for the tested coatings, the results should only be used to observe general trends. The electric fields were calculated using Macleod thin film software from a theoretical design.[21] This information then went into a transformation code for calculation of the heat generating terms needed for the finite-element thermal code TOPAZ2D.[22] The thermal results were then input into NIKE2D, a finite-element code for analyzing stresses.[23] The combination of this information is then used for modeling the multilayer failure.

Table 2 Materials properties used for the numerical calculations

Parameter	Unit	SiO_2	HfO_2	BK7
Thermal expansion coefficient	(/K)	0.7×10^{-6}	3.8×10^{-6}	7.1×10^{-6}
Thermal conductivity	(W/m/K)	1.0	4.3	1.11
Young's modulus	(GPa)	21	76	82
Density	(kg/m^3)	2,500	9,680	2,510
Heat capacity	(J/kg/K)	700	340	860
Poisson's ratio	-	0.17	0.27 (ZrO_2)	0.21
Loss tangent	S/m	.03366	1.1956	-

Design 3 has some interesting features and is representative of the other designs and was therfore used for the theoretical modeling. The overcoat thickness had a significant impact on the electric-field profile in the multilayer as illustrated in figure 5. The electric field at the outer surface of the $\lambda/7$ overcoat was at a near minimum and the field is maximized in the high index layers. The $\lambda/3$ overcoat thickness maximizes the electric field at the outer surface of the overcoat and in the coating. The electric field in the $\lambda/7 + \lambda/2$ overcoat design behaves similarly to the $\lambda/7$ overcoat design with the exception that the electric field is now maximized in the overcoat.

Calculations of the temperature differences and the significant impact of the electric field peaks in the HfO_2 layers of the coating is illustrated in figure 6. The temperature difference is further amplified by the higher absorption and lower heat capacity in the HfO_2 layers than in the SiO_2 layers. These temperature differences
lead to stresses in the multilayer as observed in figure 7. Here the small axial stress change (tensile in the outer SiO_2 layers at early times, compressive everywhere by t=20 ns) is overwhelmed in magnitude by the compressive in-plane stresses in the outer HfO_2 layers. The severe mismatch in stresses at the layer interfaces is a result of a greater than 5× higher thermal expansion coefficient of the HfO_2 layers over the SiO_2 layers.

The low damage threshold of the $\lambda/3$ overcoat can be understood by the high electric fields and thermally-induced stresses. The presence of nodular defects will only enhance these effects and thus serve as damage initiation sites.[19-20] The modeling results do not explain why delamination only occurs to the thinnest overcoat even though the stresses in the $\lambda/3$ overcoat design are 4× greater than the other designs. Also the stress profiles of the $\lambda/7$ and $\lambda/7 + \lambda/2$ overcoat designs are very similar, yet delaminations do not occur in polarizers with the thicker overcoat and the functional damage thresholds are 2-4× greater. A possible explanation is that although the model is better than just a simple electric field analysis, it unfortunately does not include a number of parameters that may have a significant impact on the stress profile. The thicker overcoat is undoubtedly a more mechanically rigid body requiring greater forces to delaminate it from the multilayer. Additionally the impacts of plasmas that modify the surface of the overcoat have not been included in the temperature profile of the overcoat.

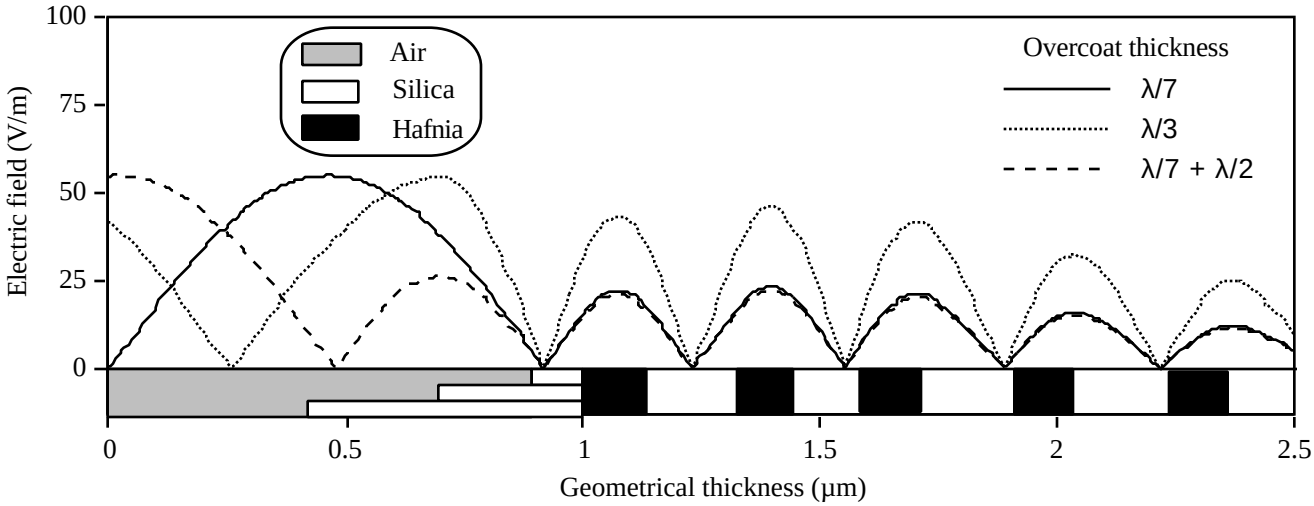

Fig. 5 Calculated electric-field distribution at "S" polarization in a Brewster's angle polarizer with λ/7, λ/3, and λ/7+ λ/2 thick overcoat at a 56° angle of incidence. The fields are plotted for an input field intensity of 1 W/m^2 measured using a detector placed normal to the beam direction.

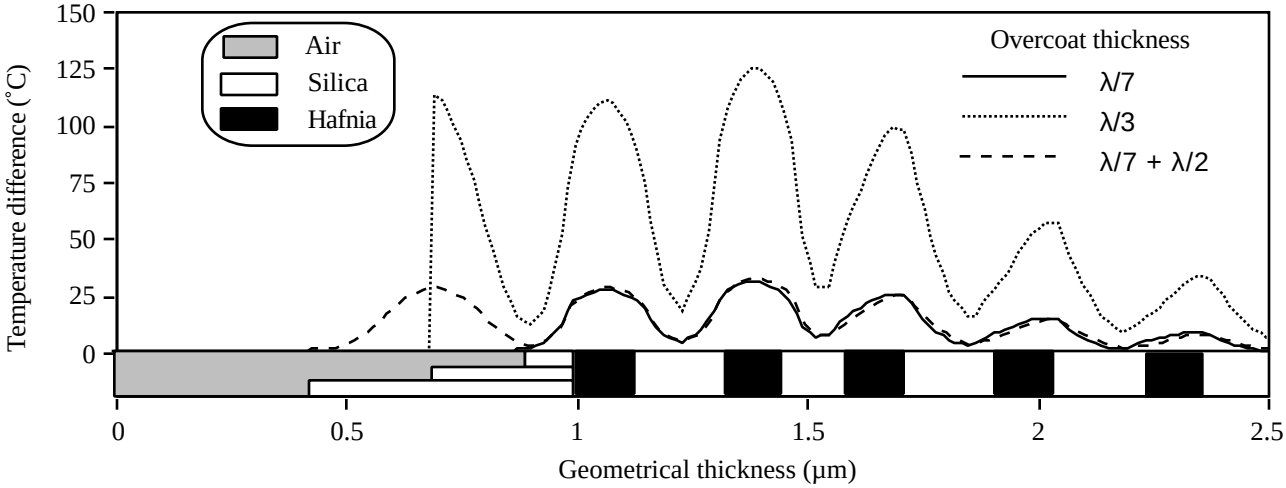

Fig. 6 Calculated temperature distribution in the polarizer at 56° for λ/7, λ/3, and λ/7+ λ/2 thick overcoat at the end of the 3-ns laser pulse for an incident fluence of 20 J/cm^2.

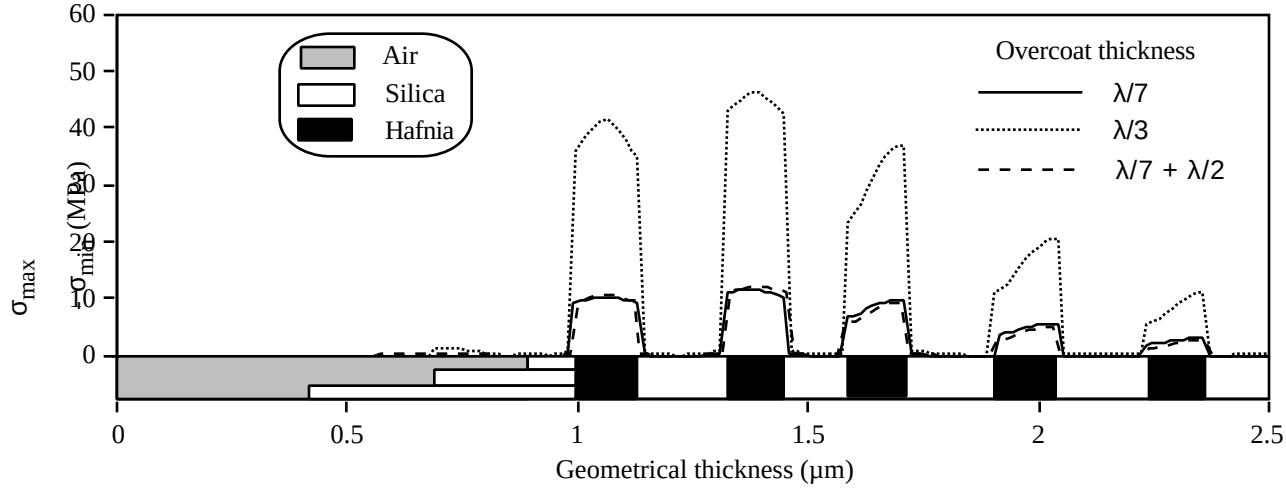

Fig. 7 Maximum principal stress (in-plane stress in this case) minus minimum principal stress (axial stress in this case) in the polarizer at 56° for λ/7, λ/3, and λ/7+ λ/2 thick overcoat at the end of the 3-ns laser pulse for an incident fluence of 20 J/cm^2.

5. SUMMARY

The damage morphology of a polarizer is significantly impacted by the presence of a SiO_2 overcoat and the thickness of the overcoat. The functional damage threshold can be increased by 2-4× by adding an additional halfwave thickness to the 0λ and λ/7 overcoat thickness designs. Electric field, temperature difference, and stress gradient profiles are useful tools for understanding some of the damage morphologies, but do not offer complete insight into the overcoat delaminations. The mechanical effects of increased overcoat thickness and the effect of plasmas on the overcoat clearly need to be measured for a greater understanding of the resultant damage morphologies.

6. ACKNOWLEDGMENTS

This work was performed under the auspices of the U.S. Department of Energy by Lawrence Livermore National Laboratory under contract No. W-7405-Eng-48.

7. REFERENCES

1. Bookless, W. A., Wheatcraft, D., "Energy & Technology Review: The National Ignition Facility," UCRL-52000-94-12 (Available from: National Technical Information Service, U.S. Department of Commerce, 5285 Port Royal Road, Springfield, Virginia 22161) 17 (1994).
2. Génin, F. Y. and Stolz, C. J., "Morphologies of laser-induced damage in hafnia-silica multilayer mirror and polarizer coatings," in *Third International Workshop on Laser Beam and Optics Characterization*, M. Morin and A. Giesen, eds., Proc. SPIE **2870**, 439-448 (1996).
3. Génin, F. Y., Stolz, C. J., Kozlowski, M. R., "Growth of laser-induced damage during repetitive illumination of HfO_2-SiO_2 multilayer mirror and polarizer coatings," in *Laser-Induced Damage in Optical Materials: 1996*, H. E. Bennett, A. H. Guenther, M. R. Kozlowski, B. E. Newnam, and M. J. Soileau, eds., Proc. SPIE **2966**, to be published.
4. Newnam, B. E., "Laser-induced-damage phenomena in dielectric films, solids and inorganic liquids," Ph. D. dissertation, Univ. of Southern California (1973).
5. Newnam, B. E., "Damage resistance of dielectric reflectors for picosecond pulses," in *Laser-Induced Damage in Optical Materials: 1974*, A. J. Glass and A. H. Guenther, eds., NIST SP **414**, 39-46 (1975).
6. Z. X. Fan, "Overcoat effect on laser-induced damage in optical coatings," Annual research report of Shanghai Institute of Optics and Fine Mechanics **3**, 120-140, (1976).
7. Carniglia C. K., J. H. Apfel, J. H., Allen, T. H., Tuttle, T. A., Lowdermilk, W. H., Milan, D., and Rainer, F., "Recent damage results on silica/titania reflectors at 1 micron," in *Laser-Induced Damage in Optical Materials: 1979*, H. E. Bennett, A. J. Glass, A. H. Guenther, and B. E. Newnam, eds., NIST SP **568**, 377-390 (1980).
8. Lowdermilk, W. H., Milam, D., and Rainer, F., "Damage to coatings and surfaces by 1.06 μm pulses," in *Laser-Induced Damage in Optical Materials: 1979*, H. E. Bennett, A. J. Glass, A. H. Guenther, and B. E. Newnam, eds., NIST SP **568**, 391-403 (1980).
9. Carniglia, C. K., "Oxide coatings for one micrometer laser fusion systems," Thin Solid Films **77**(3), 225-238 (1981).
10. Rainer, F., Lowdermilk, W. H., Milam, D., Tuttle Hart, T., Lichtenstein, T. L., and Carniglia, C. K., "Scandium oxide coatings for high-power UV laser applications," Appl. Opt. **21**(20), 3685-3688, (1982).
11. Carniglia, C. K., Tuttle Hart, T., and Staggs, M. C., "Effect of overcoats on 355 nm reflectors," in *Laser-Induced Damage in Optical Materials: 1984*, H. E. Bennett, A. H. Guenther, D. Milam, and B. E. Newnam, eds., NIST SP **727**, 285-290 (1985).
12. Wu, Z. L., Fan, Z., and Wang, Z. J., "Damage threshold dependence on film thickness," in *Laser-Induced Damage in Optical Materials: 1988*, H. E. Bennett, A. H. Guenther, B. E. Newnam, and M. J. Soileau, eds., NIST SP **775**, 321-327, (1989).
13. Wu, Z. L., Reichling, M., Fan, Z. X., and Wang, Z. J., "An understanding of the abnormal wavelength effect of overcoats," in *Laser-Induced Damage in Optical Materials: 1990*, H. E. Bennett, L. L. Chase, A. H. Guenther, B. E. Newnam, and M. J. Soileau, eds., Proc. Soc. SPIE **1441**, 200-213 (1991).
14. Walton, C. C., Génin, F. Y., Kozlowski, M. R., Loomis, G. E., and Pierce, E. "Effect of silica overlayers on laser damage of HfO_2-SiO_2 56° incidence high reflectors," in *Laser-Induced Damage in Optical Materials: 1995*, H. E. Bennett, A. H. Guenther, M. R. Kozlowski, B. E. Newnam, and M. J. Soileau, eds., Proc. SPIE **2714**, 550-558 (1996).

15.Génin, F. Y., Stolz, C. J., Reitter, T. A., Bevis, R. P., and von Gunten, M. K., "Effect of electric-field distribution on the morphologies of laser-induced damage in hafnia-silica multilayer polarizers," in *Laser-Induced Damage in Optical Materials: 1996*, H. E. Bennett, A. H. Guenther, M. R. Kozlowski, B. E. Newnam, and M. J. Soileau, eds., Proc. SPIE **2966**, to be published.
16.Sheehan, L. M., Kozlowski, M. R., Rainer, F., and Staggs, M. C., "Large area conditioning of optics for high-power laser systems," in *Laser-Induced Damage in Optical Materials: 1993*, H. E. Bennett, A. H. Guenther, L. L. Chase, B. E. Newnam, and M. J. Soileau, eds., Proc. SPIE **2114**, 333-342 (1994).
17.Morgan, A. J., Rainer, F., DeMarco, F. P., Gonzales, R. P., Kozlowski, M. R., and Staggs, M. C., "Expanded damage test facilities at LLNL," in *Laser-Induced Damage in Optical Materials: 1989*, H. E. Bennett, L. L. Chase, A. H. Guenther, B. E. Newnam, and M. J. Soileau, eds., Proc. SPIE **1438**, 47-57 (1990).
18.Bloom A. L. and Costich, V. R., "Design for high power resistance," in *Laser-Induced Damage in Optical Materials: 1975*, A. J. Glass and A. H. Guenther, eds., NIST SP **435**, 248-253 (1976).
19.DeFord, J. F. and Kozlowski, M. R., "Modeling of electric-field enhancement at nodular defects in dielectric mirror coatings," in *Laser-Induced Damage in Optical Materials: 1992*, H. E. Bennett, A. H. Guenther, L. L. Chase, B. E. Newnam, and M. J. Soileau, eds., Proc. SPIE **1848**, 455-470 (1993).
20.Sawicki, R. H., Shang, C. C., and Swatloski, T. L., "Failure characterization of nodular defects in multi-layer dielectric coatings," in *Laser-Induced Damage in Optical Materials: 1994*, H. E. Bennett, A. H. Guenther, M. R. Kozlowski, B. E. Newnam, and M. J. Soileau, eds., Proc. SPIE **2428**, 333-342 (1995).
21.Macleod, H. A., "Macleod thin-film design software," Tucson, AZ (1983).
22.Shapiro, A. B. and Edwards, A. L., "TOPAZ2D Heat transfer code users manual and thermal property database," LLNL, UCRL0ID-104558 (1990).
23.Englemann, B., "NIKE2D: a nonlinear, implicit, two-dimensional finite element code for solid mechanics, user manual," LLNL, UCRL-MA-105413 (1991).